Apr 22nd, 12:00 PM - 1:10 PM

# Dynamics and Timescales of Magmatic Processes at Cerro Uturuncu, Bolivia

Sarah Rasor
*Missouri State University*

# Dynamics and Timescales of Magmatic Processes at Cerro Uturuncu, Bolivia

**Sarah Rasor**
**Missouri State University**
**Gary S. Michelfelder, PhD**

## Abstract

Between 12-25°S latitude there is prolific volcanism fueled by the Altiplano-Puna Magmatic Body (APMB), a mid-crustal magma body above the 30° subduction of the Nazca plate and within 70-80 km thick South American crust. Cerro Uturuncu, the volcano directly above the APMB, demonstrates that the APMB experiences considerable mixing with the surrounding continental crust. Within the past 1 Ma, Uturuncu has experienced six distinct stages of andesitic to dacitic lava. With this research, we contribute greater understanding to the homogenization of and mixing within the APMB and comment on how this relates to magma residence times. The influx and recharge of new mafic material, in addition to supplementary crustal partial melt, changes the APMB composition continuously over time. While previous research on Uturuncu has focused on whole-rock geochemistry, we evaluate individual sub-crystal geochemistry and geochronometry. Major element, trace element, textural classification, and Sr diffusion modeling was performed on eight Cerro Uturuncu samples representing the four largest lava stages in Uturuncu history using the LA-ICP-MS, EPMA, optical microscopy, and Lubbers et al. (2022) trace element diffusion across plagioclase python script. Overall, we found that in the past 1 Ma, the magma chamber architecture below Cerro Uturuncu condensed while the magma itself became increasingly homogenous through mixing events. The magma was stored at or above plagioclase closure temperatures for under 1000 yrs prior to eruption.

## Introduction

Volcanoes are the surficial representation of magmatic dynamics and evolution over extensive periods of geologic time. In order to better understand volcanic events, we must first understand the root source of these events. Traditional continental arc volcanoes and mid-crustal magma bodies have been increasingly researched in recent years. However, research is lacking for irregular endmembers of continental arc volcanoes and their respective mid-crustal magma bodies.

One area of irregular continental arc volcanics can be found in the central Andes. Through various seismology studies, it was determined that subduction between 12-25°S latitude occurs at approximately 30° (Tassara et al., 2006[1]; Jordán et al., 1983[2]). The continental crust composing the back arc area in the Andes, between 12-25°S latitude, reaches thicknesses of up to 75 kilometers, a thickness only subordinate to the Tibetan plateau, making it the thickest lithospheric subduction zone on the globe (Allmendinger et al., 1997[3]). The height of the Andean orogeny and thickness of the underlying crust can be attributed to thin-skinned thrusts, lithospheric thickening from 12-10 Ma as a consequence of lithospheric cooling and shortening, as well as uplift beginning about 25 Ma (Scott et al., 2018[4]; Mamani et al., 2010[5]; Allmendinger et al., 1997; De Silva, 1989[6]; Jordán et al., 1983). The regional magma body in this area, the Altiplano Puna Magma Body (APMB), is the largest known mid-crustal magma body on the planet at an estimated 500,000 $km^3$ in volume (Ward et al., 2014[7]; Chmielowski et al., 1999[8]; Pritchard et al., 2018[9]). The unique attributes of the Central Andes warrants greater research.

Cerro Uturuncu is constructed above the center of the geophysically defined APMB and thus provides valuable insight into the assimilation of continental crust into otherwise more mafic magma origins and the overall homogenization of the APMB (Ward et al., 2014). Overall, research already completed on Uturuncu has focused on whole-rock trace element geochemistry and petrogenesis separately from Uturuncu's relationship with the evolving APMB (Pritchard et al., 2018; Michelfelder et al., 2014[10], 2013[11]). Previous studies have shown that Uturuncu lavas represent the homogenization of and concurrent crustal assimilation within the APMB (Michelfelder et al., 2014, 2013). However, it remains unclear how the homogenization affects the eruptive dynamics of Uturuncu and how residence times affect the actual homogeneity of the magma body. Integrating Uturuncu's whole-rock geochemistry and sub-crystal geochemistry with its central relationship to the APMB will provide much needed insight into the APMB's evolution over the past two million years, the APMB's inner plumbing, and Uturuncu's eruptive dynamics.

This study addresses the following two research questions: (1) How does the Altiplano-Puna Magma Body (APMB) evolve over time; and (2) How long is magma stored before eruption at Cerro Uturuncu? Through examining Uturuncu plagioclase chemistry and texture at the sub-crystal level and modeling trace element diffusion, we determine a clear picture of magma assembly, storage, and timescales within the APMB underneath Uturuncu. Trace element concentration, REE enrichment, major element concentration, and plagioclase textural analysis, was completed via laser ablation inductively coupled plasma mass spectrometer (LA-ICP-MS), electron probe microanalyzer (EPMA), and optical microscopy. These techniques helped to determine the homogenization and evolution of magma chambers below Uturuncu over time.

**Geologic Setting**

The stratovolcanic chain of the Central Andes is defined as the Andean Central Volcanic Zone (CVZ; Figure 1; de Silva, 1989; Francis and de Silva, 1989[12]). The CVZ extends from 14-28°S, overrides up to 70 km of crust, and is characterized by large volume volcanism (Godoy et al., 2017[13]; Ward et al. 2014; de Silva, 1989). The Altiplano-Puna Volcanic Complex (APVC) is found within the geologically defined boundary of the CVZ and is home to at least 20 calderas and large volcanic domes, and 50 active stratovolcanoes (Figure 1; Godoy et al., 2017; Michelfelder et al., 2013; de Silva, 1989). From 11-1 Ma, the APVC predominantly experienced expansive ignimbrite eruptions producing upwards of 15,000 $km^3$ of material (Pritchard et al., 2018; de Silva, 1989; Kussmaul et al., 1977[14]). As a result, the stratovolcanoes within the APVC boundary, including Cerro Uturuncu, are constructed upon an extensive ignimbrite base, influencing much of the material erupted within the CVZ (Michelfelder et al., 2013; de Silva, 1989).

Below the APVC, is an underlying magmatic body called the Altiplano-Puna Magmatic Body (APMB; Figure 1; Pritchard et al., 2018; Ward et al., 2014; Chmielowski et al., 1999). The APMB is a mid-crustal magma body that begins approximately 15 km below sea-level and is centered under Cerro Uturuncu (Figure 1; Ward et al., 2014). Within the past few decades, the APMB has been observed through various seismology studies aiming to image the Central Andes at depth (Ward et al., 2014; Chmielowski et al., 1999). The extensive ignimbrite eruptions within the APVC have been linked to the APMB (de Silva et al., 2006[15]). Correspondingly, APVC stratovolcanoes display petrochemical and compositional similarities to the underlying ignimbrites, suggesting

magma generation occurs in the upper crust, where the low velocity zone is found (Ward et al., 2014; Fernandez et al., 1973[16]).

While the petrochemical and geophysical data demonstrate upper crust partial melt, the area, however, is not homogeneously melted and mixed. The area of partial melt is estimated to be 500,000 $km^3$ in volume and between 4-25% melt, with the higher areas of melt increasing with proximity to the APMB center (Pritchard et al., 2018; Godoy et al., 2017; Ward et al., 2014; Chmielowski et al., 1999). Across the APVC, magma composition is only around 30% mantle-derived, which then incorporates upper crust within a mixing, assimilation, storage, and homogenization zone (MASH zone; Godoy et al., 2017; de Silva et al., 2006), with greater mantle derivation near the edges of the APMB, and more crustal assimilation toward its center (Godoy et al., 2017).

Cerro Uturuncu is a dormant Pleistocene stratovolcano in the CVZ within the boundary of the APVC and is potentially sourced by the APMB (Figure 1; Pritchard et al., 2018; Muir et al., 2015[17]; Michelfelder et al., 2014; Sparks et al., 2008[18]). Located in the southwest corner of Bolivia near the border of Chile and Argentina, Uturuncu is approximately 125 km behind the front arc of the CVZ (over 300 km inland from the Chilean coastline) which is an area volcanism is not typically seen within subduction zones (Figure 1; Michelfelder et al., 2014). Uturuncu is defined by six distinct andesitic to dacitic crystal-rich lava stages within recent geologic history (prior to 2 Ma; Muir et al., 2015; Michelfelder et al., 2014). Four of the recent stages are particularly voluminous: Puntas Negras (250-316 ka), Uturuncu (387-458 ka), Lomo Escapa (505-595 ka), and Cerro Agua de Pajarito (1016-1050 ka; Muir et al., 2015).

Cerro Uturuncu differs from the front-arc volcanoes in both location and eruptive compositions. Moho depths are approximately 35 km in the forearc and 70 km below the plateaus (Yuan et al., 2002[19]). Source magmas migrate through thicker crust under Uturuncu (~150 km) when compared to arc front volcanoes (~100 km; e.g. Aucanquilcha and Ollagüe) as evidenced by greater $K_2O$ contents which indicate greater depth to the subducting slab (Figure 1; K-h relationship; Michelfelder et al., 2013; Feeley, 1993[20]). Sr/Y ratios can be used as a proxy for crustal thickness and Moho depths (Lieu and Stern, 2019[21]). Uturuncu has a relatively low Sr/Y ratio, suggesting that the magma source occurs in a plagioclase-stable, garnet-free environment (Lieu and Stern, 2019; Michelfelder et al., 2013). Furthermore, Uturuncu lavas have higher $^{87}Sr/^{86}Sr$ ratios than front arc lavas, suggesting that crustal contamination is much more significant near the center of the APMB and/or the lavas have differing source magmas (Godoy et al., 2017; Michelfelder et al., 2014, 2013; Feeley, 1993).

**Methods**

Previously collected Uturuncu samples representing four volcanic stages suggested by Muir et al (2015) have been analyzed for $^{40}Ar/^{39}Ar$ ages, whole rock major and trace element contents, whole rock and plagioclase $^{87}Sr/^{86}Sr$ ratios, and oxygen isotope values (Michelfelder et al., 2013, 2014; Muir et al., 2015). Eight of the Uturuncu samples were chosen for in-depth sub-crystal analysis. Samples chosen for in-depth sub-crystal analysis are the following: UTGSM53, UTDM106, UTDM37, UTDM90, UTGSM69, UTDM63, UTGSM18, and UTDM112. Muir (2014, 2015) renamed the samples to only “DM” or “GSM” for brevity. Based on whole rock geochemistry, these samples are either representative of a given lava stage or vastly differ from the representative

geochemistry. Four of the samples are from the Puntas Negras stage (UTGSM53, 250 ka; UTDM106, 268 ka; UTDM37, 280 ka; UTDM90, 282 ka), two from the Uturuncu stage (UTGSM69, 387 ka; UTDM63, 455 ka), one from the Lomo Escapa stage (UTGSM18, 501 ka), and one from the Cerro Agua de Pajarito stage (UTDM112, 1001 ka; Muir et al., 2015, 2014).

For each Uturuncu sample (UTGSM53, UTDM106, UTDM37, UTDM90, UTGSM69, UTDM63, UTGSM18, UTDM112), 10 to 15 plagioclase phenocrysts were selected for major element analysis via electron microprobe at the University of Iowa and were combined with previously collected data by Michelfelder et al (2014). Major elements in plagioclase were analyzed using a JEOL JXA-8230 Superprobe (EPMA) with 5 wavelength-dispersive spectrometers and 8 large-format diffracting crystals based on the methodology described in Buckley (2022[22]). Line transects were plotted from core to rim on each selected plagioclase phenocryst. The EPMA was programmed to take a 1 μm spot every 10 μm along the transect line from plagioclase core to rim. Each spot had a 4.25 minute run-time with a 15-30 second peak dwell time and a 5 second background dwell time. Analyses were conducted at an accelerating voltage of 15 keV with a 20 nA current. Major elements for the plagioclase phenocrysts were calibrated using the Astimex standards.[43]Ca concentrations for plagioclase phenocrysts were used to determine molar anorthite percentage (%An), plagioclase zoning pattern, and as an internal standard for completing the plagioclase trace element analysis.

For each Uturuncu sample (UTDM37, UTGSM53, UTDM106, UTDM90, UTGSM69, UTDM63, UTGSM18, UTDM112), the same 10 to 15 plagioclase phenocrysts selected for major element analysis were chosen for an in-depth trace element analysis. Plagioclase phenocrysts were chosen based on the presence of zoning in XPL optical microscopy, minimal cracks and inclusions, representation of other plagioclase phenocrysts present in the sample, and adequate size of phenocrysts for analysis. The laser ablation inductively coupled mass spectrometer (LA-ICP-MS) was chosen for minor and trace element analysis as it has the needed resolution, detection limits, and allows for rapid analysis (Ginibre et al., 2007[23]; Davidson et al., 2001[24], 1999[25]). Analysis of plagioclase minor and trace elements was conducted at the University of Arkansas Trace Element and Radiogenic Isotope Lab using LA-ICP-MS. The LA-ICP-MS used is an ESI NWR 193 nm Excimer Laser Ablation System coupled with a Thermo Scientific iCapQ Quadrupole Mass Spectrometer. The following elements were analyzed for each plagioclase phenocryst: Li, Mg, Si, Sc, Ti, Cr, Fe, Zn, Rb, Sr, Y, Zr, Nb, Cs, Ba, La, Ce, Pr, Nd, Sm, Eu, Gd, Tb, Dy, Ho, Er, Tm, Yb, Lu, Hf, Pb, Th, and U. Elements were selected based on natural occurrence, isotopic occurrence, and lack of isobaric, doubly charged, and polyatomic interferences. Elements were selected based on their ability to comment on plagioclase populations, source magmas, mixing, and homogenization.

Each plagioclase phenocryst was analyzed by the LA-ICP-MS in two ways. First, by ablating 50 μm wide transect lines from core-to-rim and, second, by 50 μm diameter spots paralleling the transect. Sample UTDM37 was only analyzed with spot analysis. Line transects were scanned at 10 μm/sec. The use of transect lines with corresponding adjacent points was selected for greater data resolution for plagioclase core-to-rim transects. Statistical analysis has demonstrated that plagioclase zones grow perpendicular to the A and B axes of the crystal and are perpendicular to crystal boundaries no matter how unideal the thin section (Cheng et al., 2017[26]). Though it is worth noting that off-center sections can affect the appearance of plagioclase populations (Cheng et al.,

2017). Depending on the size of the plagioclase phenocryst, 1 to 2 transect lines were analyzed from core-to-rim. Similarly, parallel to each transect, 2-7 spots were analyzed from core-to-rim. The plagioclase phenocryst spots are classified by the spot in the center of the phenocryst, on the rim of the phenocryst, and all the spots between them, which are referred to as the "core," "rim," and "mantle," respectively. LA-ICP-MS data was reduced using the Iolite 4 software package using both NIST610 and NIST612 as external standards (Paton et al., 2011[27]; Woodhead et al., 2007[28]). Plagioclase phenocryst $^{43}Ca$ values collected with the EPMA were input as the calibration isotope within Iolite. Rare earth elements (La, Ce, Pr, Nd, Sm, Eu, Gd, Tb, Dy, Ho, Er, Tm, Yb, and Lu) were normalized to chondrite values defined by Sun and McDonough (1995)[29]. All plagioclase phenocrysts were texturally classified using optical microscopy. The optical microscope used for determining textures was the Leica DM750P microscope.

Elemental diffusion defines a crystal's residence time within the magma chamber and how much time the crystal was held at or above the closure temperature (Davidson et al., 2001; Zellmer et al., 1999[30]). Representative plagioclase phenocrysts with known spatial chemical composition have been shown to be useful in determining residence times within the magma plumbing system (Lubbers et al., 2022[31]; Costa et al., 2003[32]; Ginibre et al., 2002[33]; Davidson et al., 2007[34]; Zellmer et al., 1999). Sr is compatible with plagioclase in the upper crust, making Sr concentrations across crystal zones significant for determining residence times through diffusion modeling (Ginibre et al., 2007). To model Sr diffusion across plagioclase zones, we implemented the python script for trace element diffusion across plagioclase modeling provided by Lubbers et al. (2022). Based on Uturuncu Zircon temperatures, we use 770C as the temperature input. Spatially defined Sr and %An collected by the LA-ICP-MS and EPMA, respectively, are also inputs. Partition coefficient and trace element diffusion coefficient are determined based on the experimental paper Bindeman et al. (1998)[35] and the previously stated inputs.

**Results**

Plagioclase phenocrysts were first classified texturally to establish distinct plagioclase populations. Across all samples, notable textures include spongy cores, resorption surfaces, and sieving at the rims (also noted in Muir et al., 2014). Both the presence of and the amount of these texture types were considered. Spongy cores were seen in a majority of the plagioclase phenocrysts and most extensively in those that were relatively large (>500 μm) with considerable zoning. Resorption surfaces were present in most phenocrysts while sieved rims were observed in about half of the plagioclase phenocrysts.

Molar percent anorthite across plagioclase zones was determined for UTGSM53, UTDM106, UTDM90, and UTGSM69. UTGSM53 plagioclase zones had a range from 51.4 to 92.6 %An with an average of 66.0 %An. UTDM106 plagioclase zones had a range from 47.1 to 93.9 %An with an average of 66.4 %An.. UTDM90 plagioclase zones had a range from 60.4 to 82.6 %An with an average of 67.6 %An. UTGSM69 plagioclase zones had a range from 54.2 to 79.6 %An with an average of 63.9 %An. Molar Anorthite percentage across plagioclase zones for UTGSM53, UTDM106, UTDM90, and UTGSM69 suggest that magma with eruption ages between 387-250 ka can be characterized majoritively by oscillatory zoning and monotonous normal zoning, with a small amount of plagioclase displaying reverse zoning.

Plagioclase trace element data collected with the LA-ICP-MS is illustrated in Figure 2. Cerro Uturuncu plagioclase Fe values range from 680±40 to 11407±1968 ppm. The Fe value range increases in breadth as the stages decrease in age: Puntas Negras (316-250 ka) from 680±40 to 11407±1968 ppm; Uturuncu (458-387 ka) from 708±23 to 7542±292 ppm; Lomo Escapa (595-505 ka) from 1296±34 to 10053±1217 ppm; Cerro Agua de Pajarito (1050-1018 ka) from 1670±55 to 7439±239 ppm. Lithium, Mg, Sr, and Ba were plotted against Fe for each sample. Ranges of values for each trace element are very similar across stages, however, concentrational clustering varies. Cerro Uturuncu plagioclase Li values range from 17.3±0.998 to 153±5.15 ppm. Puntas Negras Li values range from 22.4±1.41 to 137±3.07 ppm with three distinct clusters of concentration. Uturuncu Li values range from 20.1±1.24 to 114±4.20 ppm with two distinct clusters of Li concentrations. Lomo Escapa Li values range from 51.7±2.15 to 153±5.15 ppm with one distinct cluster of Li concentration, though overall is fairly varied. Cerro Agua de Pajarito Li values range from 17.3±0.998 to 128±17.1 ppm with no notable clustering. Cerro Uturuncu plagioclase Mg values range from 54.0±1.90 to 1332±135 ppm. Puntas Negras Mg values range from 54.0±1.90 to 1332±135 ppm and display two to three distinct clusters of Mg concentration. Uturuncu Mg values range from 60.0±1.99 to 621±59.3 ppm with two distinct clusters of Mg concentration. Lomo Escapa Mg values range from 62.2±1.68 to 811±45.9 ppm and demonstrate one distinct cluster of Mg concentration, though are fairly varied overall. Finally, Cerro Agua de Pajarito Mg values range from 139±4.04 to 969±112 ppm with no notable clustering. Cerro Uturuncu plagioclase Sr values range from 379±9.07 to 2710±60.7 ppm. Puntas Negras Sr values range from 379±9.07 to 2710±60.7 ppm with two distinct clusters of Sr concentration. Uturuncu Sr values range from 799±15.4 to 2360±47.8 ppm displaying two distinct clusters of Sr concentration. Lomo Escapa Sr values range from 1233±24.8 to 2599±56.1 ppm with 1 distinct cluster of Sr concentration, though are fairly variable overall. Cerro Agua de Pajarito Sr values range from 847±16.3 to 1899±38.4 ppm showing no notable clustering. Cerro Uturuncu plagioclase Ba ranges from 47.9±1.43 to 1185±27.0 ppm. Puntas Negras Ba values range from 79.4±3.34 to 1185±27.0 ppm and exhibit two to three distinct clusters of Ba concentration. Uturuncu Ba values range from 49.1±2.07 to 838±30.1 ppm and have three distinct clusters of Ba concentration. Lomo Escapa Ba values range from 47.9±1.43 to 682±19.0 ppm and demonstrate one distinct cluster of Ba concentration, though are relatively varied overall. Lastly, Cerro Agua de Pajarito Ba values range from 66.3±2.10 to 1045±46.4 ppm with no notable clustering. It is worth noting that Puntas Negras consistently has the widest range of trace element variation for Fe, Li, Mg, Sr, and Ba.

Rare earth element (REE) data is illustrated in Figure 3. Overall, Cerro Uturuncu plagioclase has a wide variation in REE concentration with La ranging from 11.0 to 3532 ppm, Lu ranging from 0.0482 to 38.9 ppm, and Eu/Eu* ranging from 0.358 to 20.8. Puntas Negras and Cerro Agua de Pajarito both display an extensive range in REE values while Uturuncu and Lomo Escapa demonstrate a much narrower range. Puntas Negras plagioclase has two groups of REE variation, both of which contain plagioclase zones with pronounced- and low- positive Eu anomalies. The first group has high LREE/HREE ratios while the second group illustrates low LREE/HREE ratios. Samples within Puntas Negras Stage (UTGSM53, UTDM106, UTDM37, UTDM90) display one to two homogenous groups of REEs. A couple plagioclase have negative Eu anomalies which were likely inherited from an earlier stage. Most individual plagioclase have homogenous REE enrichment from core to rim, though some plagioclase exhibiting greater REE enrichment at the rim. Puntas Negras Stage plagioclase have concentrations in La ranging from 16.4 to 3532 ppm

with an average of 197 ppm, Lu ranging from 0.0482 to 38.9 ppm with an average of 0.848 ppm, and Eu/Eu* ranging from 0.358 to 18.5 with an average of 8.75. Uturuncu Stage (UTGSM69, UTDM63) plagioclase are mostly homogenous with high LREE/HREE ratios and pronounced positive Eu anomalies with few low Eu anomalies. Uturuncu Stage plagioclase have concentrations in La ranging from 76.9 to 363 ppm with an average of 170 ppm, Lu ranging from 0.0576 to 5.37 ppm with an average of 0.568 ppm, and Eu/Eu* ranging from 3.49 to 18.1 with an average of 9.01. Lomo Escapa (UTGSM18) is slightly more variable than Uturuncu stage plagioclase, though very similar overall. There is a greater range in LREE/HREE than Uturuncu with many demonstrating low Eu anomalies as well. Cores, mantles, and rims are very homogenous. Cores tend to have the lowest REE values and rims have the greatest REE values. Individual plagioclase phenocrysts exhibit an increase in REE values from core to rim as well. Lomo Escapa Stage plagioclase have concentrations in La ranging from 110 to 247 ppm with an average of 164 ppm, Lu ranging from 0.0689 to 4.99 ppm with an average of 0.758 ppm, and Eu/Eu* ranging from 3.40 to 13.7 with an average of 9.16. Cerro Agua de Pajarito (UTDM112) plagioclase is extremely variable with a significantly wide range in LREE/HREE with many demonstrating low Eu anomalies. Cores and mantles have approximately 3 and 2 distinct LREE/HREE groups, respectively. Rims tend to be more homogenous with greater amounts of REEs. Based on singular plagioclase phenocrysts, we see that cores and mantles tend to be more homogenous while rims demonstrate vastly greater amounts of REEs. Cerro Agua de Pajarito Stage plagioclase have concentrations in La ranging from 11.0 to 319 ppm with an average of 113 ppm, Lu ranging from 0.0728 to 5.26 ppm with an average of 0.791 ppm, and Eu/Eu* ranging from 3.15 to 20.79 with an average of 8.43.

Line transect trace element concentration data collected from the LA-ICP-MS concurred with the spot analysis. Most notably, across all samples (UTDM37, UTGSM53, UTDM106, UTDM90, UTGSM69, UTDM63, UTGSM18, and UTDM112) Sr and Ba concentrations mimic one another from core to rim on each plagioclase phenocryst. Mg and Fe concentrations also mimic one another from each core to rim transect.

**Discussion**

Plagioclase populations share a “common history or part of it" identified by common characteristics within zones (Ginibre et al., 2002). In that way, plagioclase populations can illustrate the different locales within the magma body and events changing magma composition below the volcano (Hughes et al., 2021[36]). Individual plagioclase populations were established by texture, major element concentration and zoning pattern, and trace element concentrations and corresponding REE enrichment.

Changes in molar anorthite percentage (%An) demonstrates the thermal and compositional evolution the plagioclase experienced over time (Ginibre et al., 2007). The pattern of which the plagioclase has experienced varying %An is referred to as the zoning pattern (Ginibre et al., 2007). Types of zoning patterns include “normal,” “reverse,” “oscillatory,” and “patchy” as defined by Ginibre et al., 2007. As UTGSM53, UTDM106, UTDM90, and UTGSM69 plagioclase can be characterized majoritively by oscillatory zoning and monotonous normal zoning, with a small amount of reverse zoning, the implications are as follows: oscillatory zoning suggests that the magma was consistently oscillating in temperature to produce the %An highs and lows within the plagioclase zones (Davidson et al., 2007; Ginibre et al., 2007); monotonous normal zoning likely precipitated during a single oscillatory period as the chamber gradually cools after a heating event

(Davidson et al., 2007; Ginibre et al., 2007). The relative highs in temperature can be attributed to an influx of new magma and/or magma mixing (Davidson et al., 2007).

Plagioclase phenocryst textures also suggest many chamber events. Spongy cores, resorption surfaces, and sieved rims indicate disequilibrium (Hughes et al., 2021; Tepley et al., 2000[37]). Spongy cores and resorption surfaces indicate a change in pressure and/or temperature suggesting an influx of new, hotter magma and/or mixing events throughout the crystals' growth histories (Tepley et al., 2000). As sieving is widely seen at the plagioclase rims, it is likely that there was an influx of new hot magma, or an increase in temperature caused by mixing that ultimately initiated the eruption (Ginibre et al., 2007, 2002; Davidson et al., 2007, 1999).

Trace element concentration was also used to distinguish and group plagioclase phenocrysts (Ginibre et al., 2007, 2002; Davidson et al., 2007, 1999). Puntas Negras stage plagioclase tend to have two to three distinct clusters of trace element compositions; Uturuncu stage plagioclase also have two to three distinct clusters; Lomo Escapa stage have one distinct cluster though trace element data is variable; Cerro Agua de Pajarito stage plagioclase have variable trace element compositions. The variability of trace elements becoming distinctly homogeneous with younger lavas demonstrates that the underlying plumbing system was likely numerous small heterogeneous bodies of partial melt during the Cerro Agua de Pajarito and Lomo Escapa stages (1050-505 ka; Figure 4). During the Lomo Escapa stage, one of the numerous chambers fed eruptions more than the others as evidenced by the minimal clustering of trace elements in this stage (Figure 4). As the plumbing system evolved, wall rock was eroded through its assimilation into the existing chambers. Eventually, the smaller chambers combined as the wall rock was partially melted between them (Figure 4). By the Uturuncu and Puntas Negras stages (458-250 ka), the underlying magma plumbing system had evolved to be two to three larger bodies of partial melt (Figure 4). These bodies were distinctly homogeneous through thorough magma mixing as evidenced by the tight and distinct trace element concentrations (Figure 4).

REEs demonstrate varying enrichment patterns and corresponding fractional crystallization (Lubbers et al., 2022; Henderson, 2013[38]; Michelfelder 2013). Varying REE enrichment across plagioclase cores, mantles, and rims suggest different growth histories with diverse degrees of enrichment (Henderson, 2013). REE data corroborates the assertion that multiple small magma chambers evolved into few larger and more homogenous bodies as Cerro Agua de Pajarito plagioclase have very variable REE concentrations with no distinct plagioclase populations (Figures 3 and 4). Magma fueling that stage was coming from many dissimilar chambers (Figure 4). As REE enrichment did increase at plagioclase rims, fractional crystallization was occurring within the chambers (Figures 3 and 4; Henderson, 2013). Lomo Escapa plagioclase REE enrichment was homogenous, suggesting that one of the many chambers primarily fueled volcanism during this period (Figures 3 and 4). As REE enrichment increases at plagioclase rims, fractional crystallization was taking place during the Lomo Escapa stage plagioclase growth as well (Figure 3; Henderson, 2013). Each of the individual samples within the Uturuncu and Puntas Negras stages exhibited 1 to 2 distinct plagioclase populations, suggesting one to two homogenous magma chambers were fueling the eruptions during this period (Figures 3 and 4). There is a slight increase in REE enrichment at plagioclase rims during these stages suggesting that fractional crystallization was occurring (Figure 3; Henderson, 2013). However, as the increase in REE

enrichment is less than what is seen in the older stages, the fractional crystallization was not as extensive (Henderson, 2013).

Plagioclase phenocrysts with overlapping texture, major element concentration and zoning pattern, and trace element concentrations and corresponding LREE to HREE ratios are considered a population (Ginibre et al., 2007, 2002; Davidson et al., 2007). Each growth history subsequently commented on different magma chamber locales and the evolution of the chambers over time. Overall, Puntas Negras (316-250 ka) and Uturuncu (458-387 ka) can each be characterized by two distinctly homogeneous plagioclase populations; Lomo Escapa (595-505 ka) by one distinct plagioclase population with other populations being varied; Cerro Agua de Pajarito (1050-1018 ka) by many heterogeneous plagioclase populations. The magma architecture below Cerro Uturuncu evolved from many heterogeneous chambers to larger homogeneous bodies over Cerro Uturuncu's eruptive history (Figure 4).

Approximately 10 to 15 plagioclase phenocrysts in four of the five most recent samples (UTGSM53, UTDM106, UTDM90, and UTGSM69) were selected for Sr diffusion modeling using the diffusion modeling code published by Lubbers et al. (2022). Results indicate that average residence times are 1488.8 years for UTGSM53, 351.5 years for UTDM106, 220.7 years for UTDM90, and 203.3 years for UTGSM69. Consequently, the average residence time for Puntas Negras stage is 721.3 years while Uturuncu stage is 203.3 years. For geologic timescales, these residence times are relatively short. Magma residence time and eruption ages are shown in Figure 5.

**Conclusion**

The use of sub-crystal analysis helped in visualizing the evolution of the magma chamber architecture below Cerro Uturuncu over its eruptive history. Optical microscopy, LA-ICP-MS, and EPMA analysis allowed for detailed plagioclase growth history evaluation. Plagioclase textures suggested there were many new magma influxes and/or mixing events to cause an increase in temperature and corresponding disequilibrium. Overall, the Altiplano Puna Manga Body below Cerro Uturuncu has experienced chamber consolidation and homogenization. From 1001 to 250 ka, the magma structure shifted from many compositionally diverse isolated chambers to a few compositionally homogeneous chambers. This evolution of the magma plumbing architecture is evidenced by changing trace element clustering and REE enrichment across four of Cerro Uturuncu's eruptive stages. Puntas Negras (316-250 ka) demonstrated two distinctly homogeneous plagioclase populations through trace element and REE analysis. Each individual sample within Puntas Negras stage had one to two of those plagioclase populations suggesting that the two chambers erupting did not always do so at the same time. Uturuncu (458-387 ka) could also be characterized by two plagioclase populations. These populations erupted from two chambers that were well-mixed and distinctly homogeneous. Lomo Escapa (595-505 ka) had one distinct plagioclase population, though plagioclase was varied overall. During the Lomo Escapa stage, there were many poorly-mixed magma chambers. It is likely that, because there is one distinct plagioclase population, material was mainly erupted from one chamber. Cerro Agua de Pajarito (1050-1018 ka) had no distinct plagioclase populations and displayed widely varied trace element concentrations and REE enrichment. Material from the Cerro Agua de Pajarito stage erupted from many unevolved and poorly-mixed, heterogenous chambers. Fractional crystallization occurred throughout Cerro Uturuncu's history. Magma was stored for relatively short periods of time prior

to eruption. Diffusion modeling of Sr across plagioclase zones suggests that Puntas Negras Stage plagioclase resided in magma chambers on average for approximately 721.3 years prior to eruption while Uturuncu stage plagioclase resided in the chamber on average for about 203.3 years prior to eruption. Given the extensivity of spongy cores, resorption surfaces, and sieved rims, the plagioclase spent additional time within the chamber under conditions not conducive of crystal growth.

**Figures**

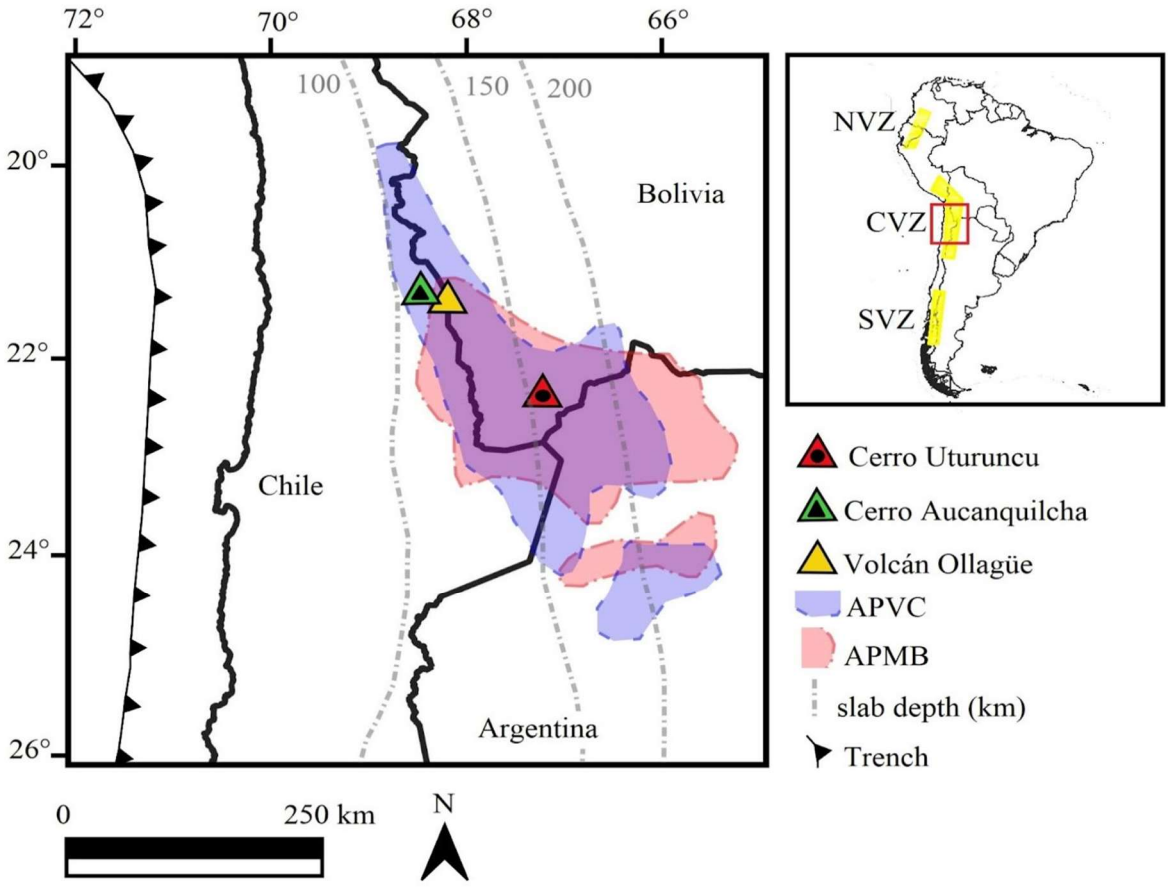


**Figure 1. Regional map of Cerro Uturuncu with respect to two front arc volcanoes, Cerro Aucanquilcha and Volcán Ollagüe, within the Andean Central Volcanic Zone (CVZ). The approximate boundary of the Altiplano Puna Volcanic Complex (APVC) and Altiplano Puna Magma Body (APMB) are outlined. Modified from Muir et al. (2014).**

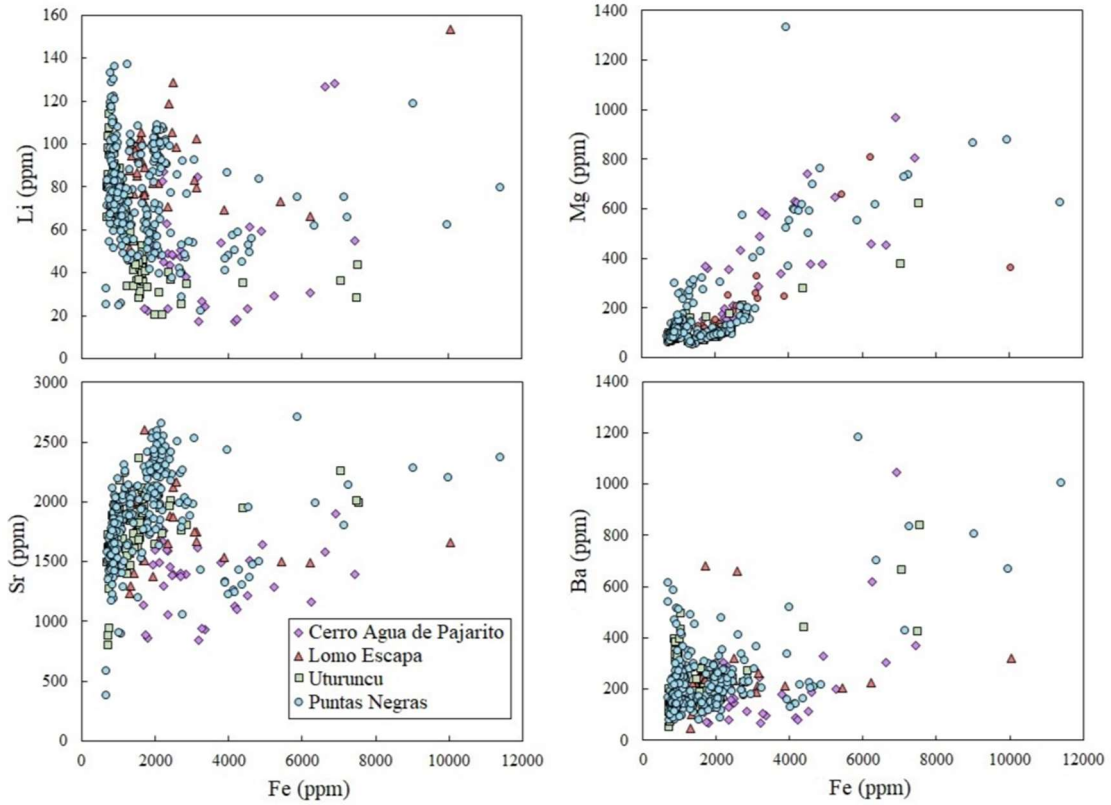


**Figure 2. Trace element comparison (Li, Mg, Sr, and Ba versus Fe) of Cerro Agua de Pajarito, Lomo Escapa, Uturuncu, and Puntas Negras stages.**

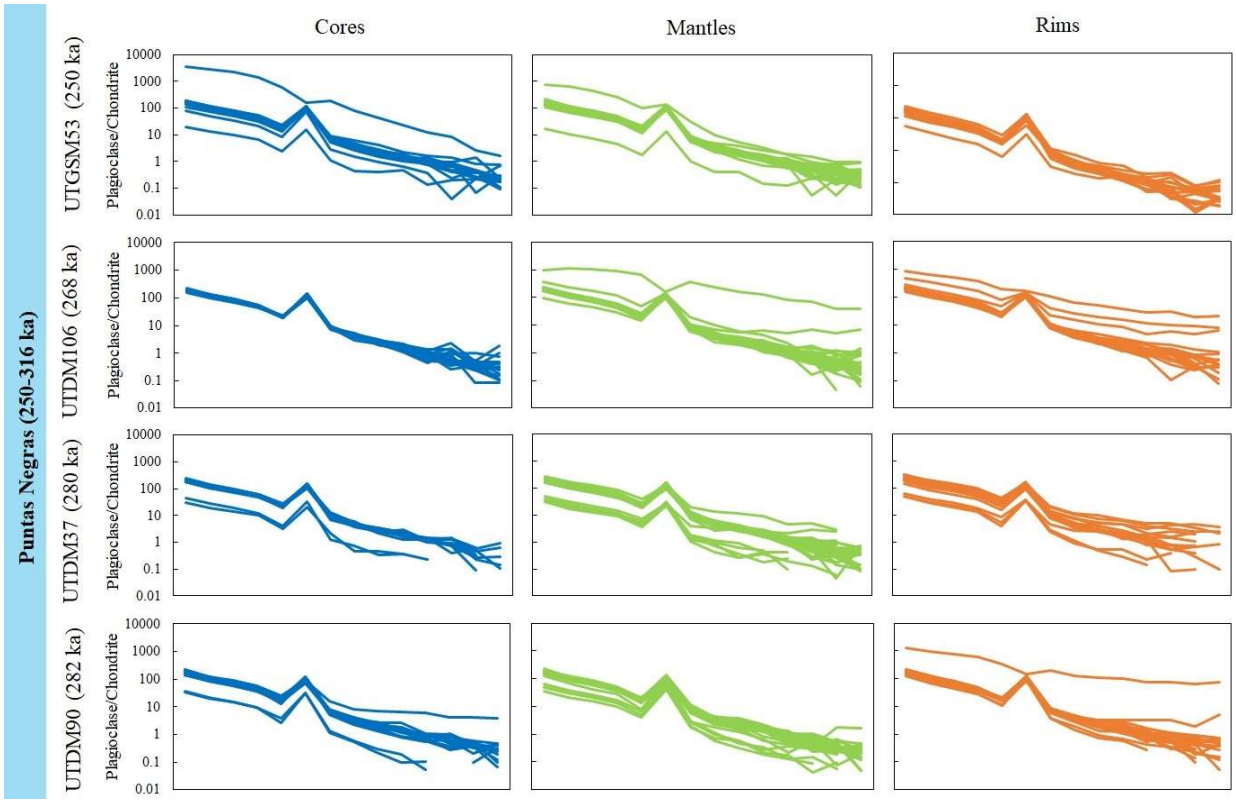

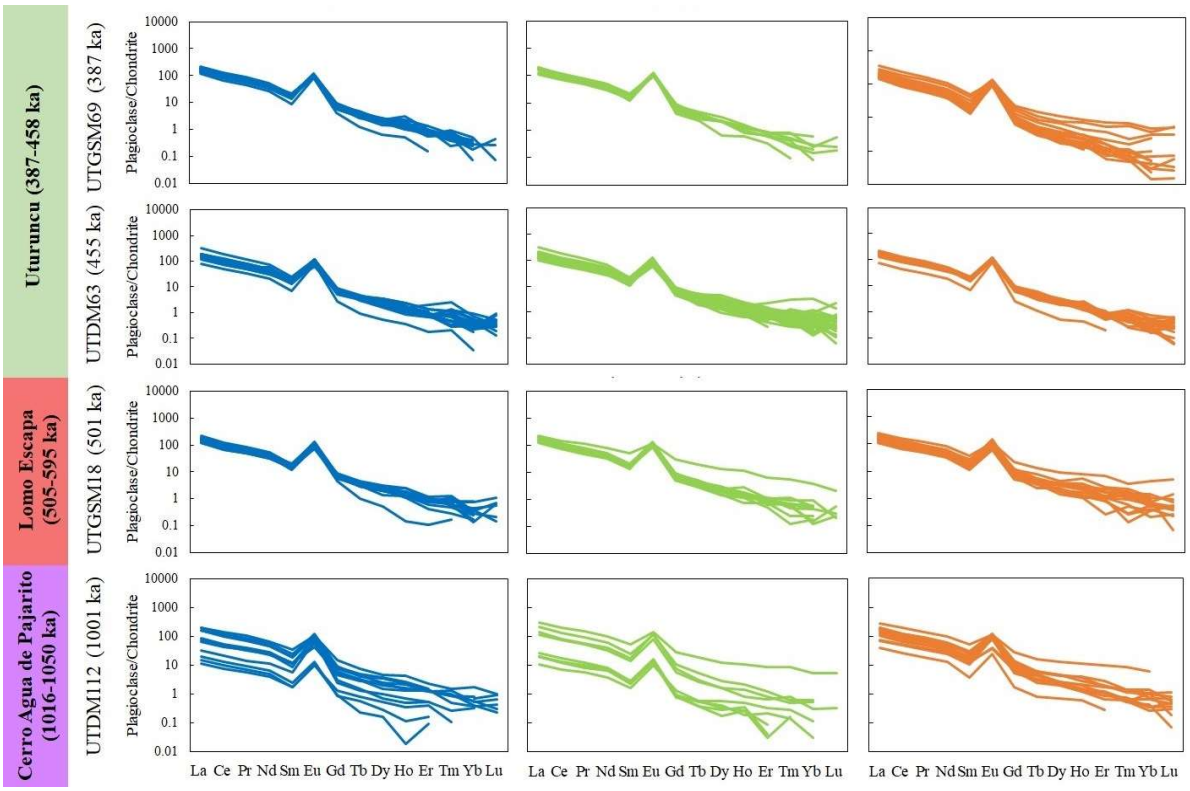


**Figure 3. REE diagram for Puntas Negras samples (UTGSM53, UTDM106, UTDM37, and UTDM90), Cerro Agua de Pajarito sample (UTDM112), Lomo Escapa sample (UTGSM18), and Uturuncu samples (UTGSM69 and UTDM63) separated into cores, mantles, and rims.**

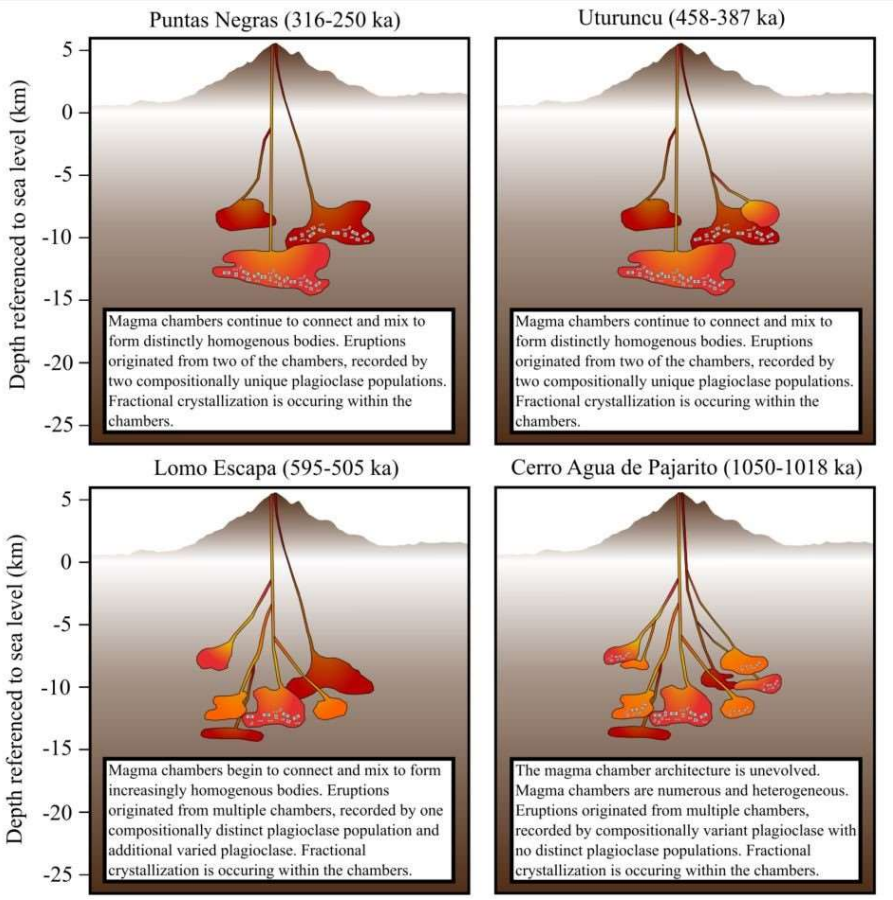


**Figure 4. Proposed underlying magma plumbing architecture for Cerro Uturuncu. From 1050 ka to 250 ka, the magma chambers evolve from many heterogeneous bodies to few individually homogenous bodies. Fractional crystallization occurs within these bodies throughout its history.**

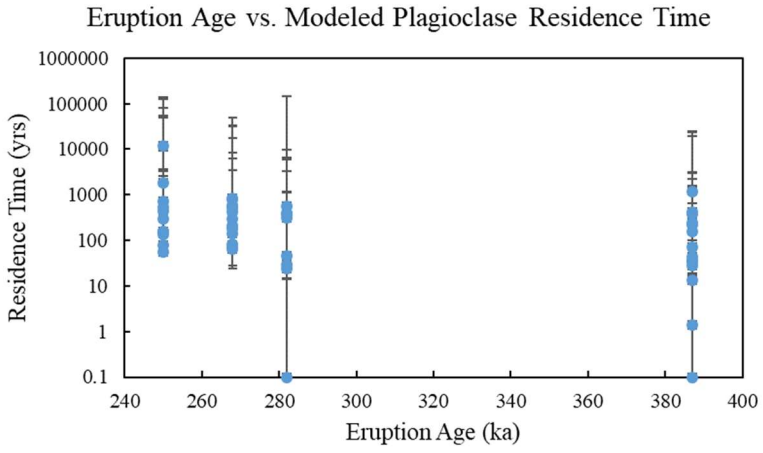


**Figure 5. Sr diffusion modeling residence times at 770C for samples UTGSM53, UTDM106, UTDM90, and UTGSM69. Error bars indicate 2σ values.**

## Acknowledgements

I would like to thank my advisor, Dr. Gary Michelfelder, for his consistent guidance and feedback throughout this research as well as my thesis committee members Dr. Mélida Guitiérrez and Dr. Kevin Mickus for their support. I am grateful to the NASA-Missouri Space Grant Consortium (Grant Award 80NSSC20M0100), the National Science Foundation, and the Missouri State University Graduate College for making this research possible. I would also like to acknowledge Barry Shaulis and Kenny Horkley for advising me on using the analytical instruments at their respective institutions (LA-ICP-MS, University of Arkansas; EPMA, University of Iowa). Finally, I would like to thank my student colleagues, Nathan Lenhard, César Bucheli-Olaya, Bennett Van Horn, Chris Willingham, and Joseph Lane, family, and friends for their help and support.

## References

(1) Tassara, A., Götze, H.J., Schmidt, S., and Hackney, R., 2006, Three-dimensional density model of the Nazca plate and the Andean continental margin: Journal of Geophysical Research: Solid Earth, v. 111.
(2) Jordán, T.E., Isacks, B.L., Allmendinger, R.W., Brewer, J.A., Ramos, V.A., and Ando, C.J., 1983, Andean tectonics related to geometry of subducted Nazca plate: Geological Society of America Bulletin, v. 94, p. 341-361.
(3) Allmendinger, R.W., Jordan, T.E., Kay, S.M., and Isacks, B.L., 1997, The evolution of the Altiplano-Puna plateau of the Central Andes: Annual review of earth and planetary sciences, v. 25, p. 139-174.
(4) Scott, E.M., Allen, M.B., Macpherson, C.G., McCaffrey, K.J., Davidson, J.P., Saville, C. and Ducea, M.N., 2018, Andean surface uplift constrained by radiogenic isotopes of arc lavas: Nature communications, v. 9, p.1-8.
(5) Mamani, M., Wörner, G., and Sempere, T., 2010, Geochemical variations in igneous rocks of the Central Andean orocline (13 S to 18 S): Tracing crustal thickening and magma generation through time and space: GSA Bulletin, v. 122, p. 162-182.
(6) De Silva, S.L., 1989, Altiplano-Puna volcanic complex of the central Andes: Geology, v. 17(12), p. 1102-1106.
(7) Ward, K.M., Zandt, G., Beck, S.L., Christensen, D.H. and McFarlin, H., 2014, Seismic imaging of the magmatic underpinnings beneath the Altiplano-Puna volcanic complex from the joint inversion of surface wave dispersion and receiver functions: Earth and Planetary Science Letters, v. 404, p. 43-53.
(8) Chmielowski, J., Zandt, G., and Haberland, C., 1999, The central Andean Altiplano-Puna magma body: Geophysical Research Letters, v. 26, p. 783-786.
(9) Pritchard, M.E., De Silva, S.L., Michelfelder, G., Zandt, G., McNutt, S.R., Gottsmann, J., West, M.E., Blundy, J., Christensen, D.H., Finnegan, N.J., and Minaya, E., 2018, Synthesis: PLUTONS: Investigating the relationship between pluton growth and volcanism in the Central Andes: Geosphere, v. 14, p. 954-982.
(10) Michelfelder, G.S., Feeley, T.C., and Wilder, A.D., 2014, The volcanic evolution of Cerro Uturuncu: A high-K, composite volcano in the back-arc of the Central Andes of SW Bolivia: International Journal of Geosciences, v. 5, p. 1263.
(11) Michelfelder, G.S., Feeley, T.C., Wilder, A.D., and Klemetti, E.W., 2013, Modification of the continental crust by subduction zone magmatism and vice-versa: Across-strike geochemical variations of silicic lavas from individual eruptive centers in the Andean Central volcanic zone: Geosciences, v. 3, p. 633-667.
(12) Francis, P.W. and De Silva, S.L., 1989, Application of the Landsat Thematic Mapper to the identification of potentially active volcanoes in the Central Andes: Remote Sensing of Environment, v. 28, p. 245-255.
(13) Godoy, B., Wörner, G., Le Roux, P., de Silva, S., Parada, M.Á., Kojima, S., González-Maurel, O., Morata, D., Polanco, E. and Martínez, P., 2017, Sr-and Nd-isotope variations along the Pleistocene San Pedro–Linzor volcanic chain, N. Chile: Tracking the influence of the upper crustal Altiplano-Puna Magma Body: Journal of Volcanology and Geothermal Research, v. 341, p. 172-186.
(14) Kussmaul, S., Hörmann, P.K., Ploskonka, E., and Subieta, T., 1977, Volcanism and structure of southwestern Bolivia: Journal of Volcanology and Geothermal Research, v. 2, p.73-111..
(15) De Silva, S., Zandt, G., Trumbull, R., Viramonte, J.G., Salas, G. and Jiménez, N., 2006, Large ignimbrite eruptions and volcano-tectonic depressions in the Central Andes: a thermomechanical perspective: Geological Society, v. 269, p. 47-63.
(16) Fernandez, A.C., Hörmann, P.K., Kussmaul, S., Meave, J., Pichler, H., and Subieta, T., 1973, First petrologic data on young volcanic rocks of SW-Bolivia: Tschermaks mineralogische und petrographische Mitteilungen, v. 19, p. 149-172.
(17) Muir, D. D., Barfod, D.N., Blundy, J.D., Rust, A.C., Sparks, R.S.J., and Clarke, K.M., 2015, The Temporal Record of Magmatism at Cerro Uturuncu, Bolivian Altiplano: Geological Society, London, Special Publications, v. 422, p. 57–83.
(18) Sparks, R.S.J., Folkes, C.B., Humphreys, M.C., Barfod, D.N., Clavero, J., Sunagua, M.C., McNutt, S.R., and Pritchard, M.E., 2008, Uturuncu volcano, Bolivia: Volcanic unrest due to mid-crustal magma intrusion: American Journal of Science, v. 308, p. 727-769..
(19) Yuan, X., Sobolev, S.V., and Kind, R., 2002, Moho topography in the central Andes and its geodynamic implications: Earth and Planetary Science Letters, v. 199, p. 389-402.
(20) Feeley, T.C., 1993, Crustal modification during subduction-zone magmatism: evidence from the southern Salar de Uyuni region (20-22 S), central Andes: Geology, v. 21, p. 1019-1022.

(21) Lieu, W.K. and Stern, R.J., 2019, The robustness of Sr/Y and La/Yb as proxies for crust thickness in modern arcs: Geosphere, v. 15, p. 621-641.
(22) Buckley, K.L., 2022, Aucanquilcha Volcanic Cluster Magma Evolution and Magma Plumbing System Architecture During the Gordo Stage (6-4 Ma).
(23) Ginibre, C., Wörner, G., and Kronz, A., 2007, Crystal zoning as an archive for magma evolution: Elements, v. 3, p. 261-266.
(24) Davidson, J., Tepley III, F., Palacz, Z., and Meffan-Main, S., 2001, Magma recharge, contamination and residence times revealed by in situ laser ablation isotopic analysis of feldspar in volcanic rocks: Earth and Planetary Science Letters, v. 184, p. 427-442.
(25) Davidson, J.P., Tepley III, F.J., Palacz, Z. and Meffan-Main, S., 1999, August. Crystal Isotopic Stratigraphy Using Laser Ablation: In Ninth Annual VM Goldschmidt Conference, p. 7141.
(26) Cheng, L., Costa, F. and Carniel, R., 2017, Unraveling the presence of multiple plagioclase populations and identification of representative two-dimensional sections using a statistical and numerical approach: American Mineralogist: Journal of Earth and Planetary Materials, v. 102(9), p.1894-1905.
(27) Paton, C., Hellstrom, J., Paul, B., Woodhead, J. and Hergt, J., 2011, Iolite: Freeware for the visualisation and processing of mass spectrometric data: Journal of Analytical Atomic Spectrometry, v. 26, p. 2508-2518.
(28) Woodhead, J.D., Hellstrom, J., Hergt, J.M., Greig, A. and Maas, R., 2007, Isotopic and elemental imaging of geological materials by laser ablation inductively coupled plasma-mass spectrometry: Geostandards and Geoanalytical Research, v. 31, p. 331-343.
(29) McDonough, W.F. and Sun, S.S., 1995, The composition of the Earth: Chemical geology, v. 120, p. 223-253.
(30) Zellmer, G.F., Blake, S., Vance, D., Hawkesworth, C., and Turner, S., 1999, Plagioclase residence times at two island arc volcanoes (Kameni Islands, Santorini, and Soufriere, St. Vincent) determined by Sr diffusion systematics: Contributions to Mineralogy and Petrology, v. 136, p.345-357.
(31) Lubbers, J., Kent, A.J. and de Silva, S., 2022, Thermal budgets of magma storage constrained by diffusion chronometry: the Cerro Galán ignimbrite: Journal of Petrology, v. 63(7).
(32) Costa, F., Chakraborty, S., and Dohmen, R., 2003, Diffusion Coupling between Trace and Major Elements and a Model for Calculation of Magma Residence Times Using Plagioclase: Geochimica Et Cosmochimica Acta, v. 67, p. 2189–2200.
(33) Ginibre, C., Wörner, G., and Kronz, A., 2002, Minor-and trace-element zoning in plagioclase: implications for magma chamber processes at Parinacota volcano, northern Chile: Contributions to Mineralogy and Petrology, v. 143, p. 300-315.
(34) Davidson, J.P., Morgan, D.J., and Charlier, B.L., 2007, Isotopic microsampling of magmatic rocks: Elements, v. 3, p. 253-259.
(35) Bindeman, I.N., Davis, A.M. and Drake, M.J., 1998, Ion microprobe study of plagioclase-basalt partition experiments at natural concentration levels of trace elements: Geochimica et Cosmochimica Acta, v. 62, p.1175-1193.
(36) Hughes, G.E., Petrone, C.M., Downes, H., Varley, N.R., and Hammond, S.J., 2021, Mush remobilisation and mafic recharge: A study of the crystal cargo of the 2013–17 eruption at Volcán de Colima, Mexico: Journal of Volcanology and Geothermal Research, v. 416, p. 107296.
(37) Tepley III, F.J., Davidson, J.P., Tilling, R.I. and Arth, J.G., 2000, Magma mixing, recharge and eruption histories recorded in plagioclase phenocrysts from El Chichon Volcano, Mexico: Journal of Petrology, v. 41(9), p. 1397-1411.
(38) Henderson, P., 2013, Rare earth element geochemistry: Elsevier.

## Biography

My name is Sarah Rasor and this research has been completed in conjunction with my studies as a M.Sc. Geology student at Missouri State University's Department of Geography, Geology and Planning advised by Dr. Gary Michelfelder. I was born and raised in San Clemente, California, a small town on the Southern California coast and I hope to become an earth sciences teacher.